J Biomol NMR (2014) 60:197–202
DOI 10.1007/s10858-014-9860-0

NMR STRUCTURE NOTE

Solution structure of a C-terminal fragment (175–257) of CV_0373 protein from *Chromobacterium violaceum* adopts a winged helix-turn-helix (wHTH) fold

Yunhuang Yang · Theresa A. Ramelot · Hsiau-Wei Lee · Rong Xiao · John K. Everett · Gaetano T. Montelione · James H. Prestegard · Michael A. Kennedy

Received: 30 July 2014 / Accepted: 28 August 2014 / Published online: 1 October 2014

Biological context

Chromobacterium violaceum, a Gram-negative β-proteobacterium, is a species of free-living microorganisms found in soil and water. In addition to providing fundamental insights into environmental adaption strategies, genomes of these bacteria can also provide a rich source of genes with biotechnological potential and medical utility. For instance, *C. violaceum* produces a natural antibiotic called violaceine that has been shown to be useful for the treatment of colon and other cancers (Kodach et al. 2006). The complete genome sequence of *C. violaceum* was identified by the Brazilian National Genome Sequencing Consortium in 2003 (Brazilian National Genome Project 2003). Their study showed that there were 4,431 uniformly distributed predicted protein coding ORFs, and 958 (21.6 %) of these were identified as conserved hypothetical proteins. Among them, protein CV_0373 from *C. violaceum* (UniProtKB entry Q7P141, gi 34101683, KEGG entry cvi:CV_0373) is annotated as a conserved hypothetical protein with unknown structure and function. Information based on genomic context provided no insight into its biochemical or biological functions. CV_0373 contains two domains (http://www.kegg.jp/ssdb-bin/ssdb_motif?kid=cvi:CV_0373): an N-terminal domain (5–139) belonging to the NYN domain family, and a C-terminal domain (182–246) belonging to the OST–HTH/LOTUS domain family. Both domains are widely conserved in eukaryotes and bacteria. When CV_0373 was selected as a target for structure determination in 2009 by the Northeast Structural Genomics Consortium (NESG) (NESG ID CvR118A), there were no structural representative for either domain family.

NYN domains (PF01936, http://pfam.sanger.ac.uk/family/pf01936) have been identified as putative novel ribonuclease domains by using sequence profile searches and contextual information (Anantharaman and Aravind 2006), and were named after members found in eukaryotic proteins typified by the Nedd4-binding protein I and the bacterial YacP-like proteins (*N*edd4-BPI, *Y*acP *n*ucleases: NYN domains). In 2010, OST–HTH domains (PF12872, http://pfam.sanger.ac.uk/family/12872) were predicted to be RNA-binding domains based on contextual information from domain architectures, sequence-structure superpositions, and available functional information (Anantharaman et al. 2010). This conserved domain, which adopts a winged helix-turn-helix (wHTH) fold, was found in the RNA-binding protein Oskar in *Drosophia* and the vertebrate nuage complex proteins TDRD5 and TDRD7. The protein was therefore named as *Os*kar-*T*DRD5/TDRD7 HTH (OST–HTH) and is predicted to bind to dsRNA. This domain is also referred to as a LOTUS domain, named

Y. Yang · T. A. Ramelot · M. A. Kennedy (✉)
Department of Chemistry and Biochemistry, and the Northeast Structural Genomics Consortium, Miami University, Oxford, OH 45056, USA
e-mail: kennedm4@miamioh.edu

H.-W. Lee · J. H. Prestegard
Complex Carbohydrate Research Center, and the Northeast Structural Genomics Consortium, University of Georgia, Athens, GA 30602, USA

R. Xiao · J. K. Everett · G. T. Montelione
Department of Molecular Biology and Biochemistry, and the Northeast Structural Genomics Consortium, Center for Advanced Biotechnology and Medicine, Rutgers, The State University of New Jersey, Piscataway, NJ 08854, USA

G. T. Montelione
Department of Biochemistry, Robert Wood Johnson Medical School, University of Medicine and Dentistry of New Jersey, Piscataway, NJ 08854, USA

after Limkain, Oskar and TUdor-containing proteins 5 and 7, or TDRD5 and TDRD7 (Callebaut and Mornon 2010).

In eukaryotes, NYN domains were found in several distinctive multi-domain architectures showing fusions with various other RNA-binding domains, suggesting functionally diverse roles (Anantharaman and Aravind 2006). Interestingly, the multi-domain architectures of proteins containing OST–HTH domains suggested that this domain may be crucial to the recognition and localization of dsRNA such as miRNAs, rasiRNAs and piRNAs hybridized to their targets (Anantharaman et al. 2010). By contrast, based on conserved genetic context (Anantharaman and Aravind 2006), bacterial versions of the NYN domain were deduced to be potential components of the processome/degradsome that processes tRNAs or ribosomal RNAs. Bacterial versions of the OST–HTH domain are often found in multi-domain architectures with single or tandem OST–HTH domains fused to an N-terminal NYN domain. These genes (NYN + OST–HTH) were not found in gene clusters that could be linked to any other known RNA-processing system in bacteria. Hence, OST–HTH domains might recruit substrates for processing or degradation, with these bacterial proteins functioning as standalone RNA-degradation enzymes (Anantharaman et al. 2010).

In this study, we present the solution structure of a C-terminal fragment (175–257) of CV_0373 (referred to as CV_0373 CTD) from *C. violaceum*. The solution structure of this C-terminal domain adopts a wHTH fold, and exhibits a HTH core that is conserved in bacterial and eukaryotic homologs based on ConSurf analysis (Ashkenazy et al. 2010; Glaser et al. 2003). Structure analysis of CV_0373 CTD hints that its function may be involved in dsRNA binding.

Methods and results

Protein expression, purification and NMR samples preparation

Full length *CV_0373* gene of *C. violaceum* encodes 297 amino acids. The selected fragment of the *CV_0373* gene was cloned into a pET21-based expression vector to encode the 83-residue CV_0373 CTD (175–257) including a short C-terminal hexaHis tag (LEHHHHHH). Following NESG standard protocols (Acton et al. 2011), the CV_0373 CTD was expressed and purified to prepare U-^{13}C, ^{15}N (NC) and U-^{15}N, 5 % biosynthetically directed ^{13}C (NC5) samples. NMR samples were purified using an ÄKTAxpress (GE Healthcare) with a Ni-affinity column (HisTrap HP IMAC column, 5 ml) followed by gel filtration chromatography (HiLoad 26/60 Superdex 75). The protein was concentrated to a final concentration of 0.8–0.9 mM in the NMR buffer containing 10 % v/v D_2O: 20 mM NH_4OAc, 100 mM NaCl, 5 mM $CaCl_2$, 10 mM DTT, and 0.02 % NaN_3 at pH 4.5. A D_2O-exchanged sample was prepared for H–D exchange experiments by freezing the NC sample followed by lyophilization and resuspension in 99.9 % D_2O (Acros Organics).

NMR spectroscopy data collection and assignments

NMR experiments were carried out at 298 K on Varian Inova 600 MHz spectrometer with a 5-mm HCN cryogenic probe and Bruker Avance III 850 MHz spectrometer equipped with a conventional room temperature 5-mm HCN probe. ^{1}H, ^{13}C, and ^{15}N chemical shifts were assigned from conventional triple-resonance spectra on NC sample including 2D ^{1}H-^{15}N HSQC and ^{1}H-^{13}C HSQC (aliphatic and aromatic), 3D HNCO, HNCA, HN(CO)CA, HNCACB, CBCA(CO)NH, HBHA(CO)NH, HC(C)H-COSY, HC(C)H-TOCSY and (H)CCH-TOCSY. Stereospecific isopropyl methyl assignments for all Val and Leu amino acids were deduced from characteristic cross-peak fine structures in a high resolution 2D ^{1}H-^{13}C HSQC spectrum of NC5 sample (Neri et al. 1989). To obtain the NOE-based distance restraints required for structure calculations, four NOESY spectra including 3D ^{15}N-edited NOESY–HSQC and ^{13}C-edited NOESY–HSQC (optimized for aliphatic or aromatic carbons) on the NC sample, and an additional 4D ^{13}C-^{13}C-HMQC–NOESY–HMQC on the D_2O-exchanged sample (99.9 % D_2O) were collected with a 70 ms mixing time. These NOESY spectra were also analyzed to confirm side chain ^{1}H assignments. All NMR data were processed using NMRPipe program and analyzed with the Sparky program. The 2D ^{1}H-^{15}N HSQC spectrum of CV_0373 CTD was well dispersed and almost completely assigned (Fig. 1). Final ^{1}H, ^{13}C and ^{15}N chemical shifts were deposited in the BioMagResBank (BMRB ID 17020).

Residual dipolar coupling

Backbone ^{1}H-^{15}N residual dipolar couplings (RDCs) for CV_0373 CTD were measured on isotropic and aligned NC5 samples in 2D *J*-modulated spectra on a Varian Inova 600 MHz spectrometer at 298 K (Tjandra et al. 1996). The protein was partially aligned in two alignment media $C_{12}E_5$ polyethylene glycol (PEG) and positively charged compressed polyacrylamide gel (Hansen et al. 1998; Ruckert and Otting 2000). In total, 91 RDC restraints (42 from PEG and 49 from Gel) were used for the final structure refinement calculations.

NMR structure calculation and refinement

NOE-based inter-proton distance restraints were determined automatically for CV_0373 CTD using CYANA 2.1

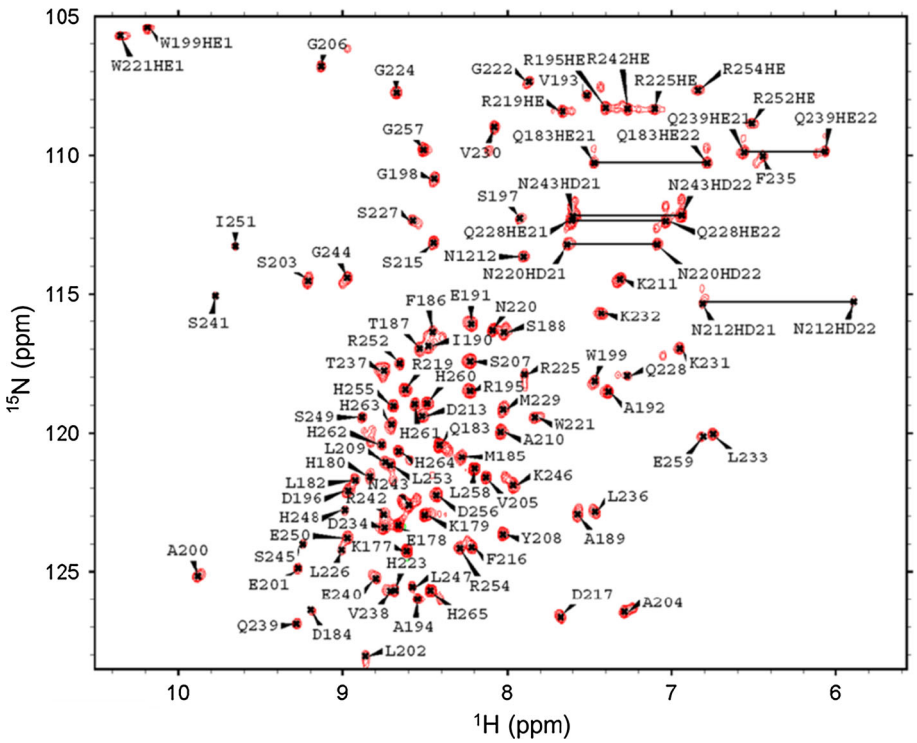

Fig. 1 Assigned ^{1}H-^{15}N HSQC spectrum of ^{13}C, ^{15}N-labeled CV_0373 CTD (0.9 mM) in NMR buffer collected at 298 K. Assigned side chain resonances of Arg ($H^{\varepsilon}/N^{\varepsilon}$, aliased), Trp199 and Trp221 ($H^{\varepsilon 1}/N^{\varepsilon 1}$, aliased), and side chain resonances of Asn and Gln (Asn $H^{\varepsilon 2}/N^{\varepsilon 2}$, and Gln $H^{\varepsilon 2}/N^{\varepsilon 2}$) are indicated (*lines*)

(Guntert 2004). Input for CYANA consisted of chemical shift assignments, NOESY peak lists from four NOESY spectra with peak intensities, and the restraints for backbone phi (φ) and psi (ψ) torsion angle derived from chemical shifts of backbone atoms using the TALOS+ software program (Shen et al. 2009). Manual and iterative refinements of NOESY peak picking lists were guided using NMR RPF quality to assess "goodness of fit" between calculated structures and NOESY peak lists (Huang et al. 2005). Towards the end of the iterative structure calculation process, 29 × 2 hydrogen bond restraints for the NH–O and N–O distances were introduced based on proximity of donor and receptor in early structure calculations and confirmation from deuterium exchange measurements. The final modified NOE-based inter-proton distance restraints, dihedral angle restraints, and hydrogen bond restraints were converted to Xplor format using PDBStat (Bhattacharya et al. 2007) with an increase of 10 % to the upper bounds for the NOE restraints for structure calculations. These restraints were used to calculate 100 structures using Xplor-NIH version 2.25 with a standard simulated annealing protocol (Schwieters et al. 2006) followed by refinement of the 20 lowest energy structures including two sets of NH RDCs using Xplor+ protocols (Cai et al. 2007). The final NMR ensemble of 20 structures with the lowest energy has been deposited in the RCSB Protein Data Bank (PDB ID 2KZV). Structural statistics and global structure quality factors were computed using PSVS version 1.4 (Table 1) (Bhattacharya et al. 2007).

Solution structure of CV_0373 CTD

CV_0373 CTD has a molecular weight of 10.6 kDa (including the 8-residue C-terminal tag). Analytical static light scattering measurements in-line with gel-filtration chromatography indicated that it was a monomer under the conditions used in the NMR experiments. The estimated overall isotropic rotational correlation time (τ_c) of 6.1 ± 0.5 ns at 298 K, derived from ^{15}N relaxation times determined from 1D ^{15}N-edited T_1 and T_2 experiments (Kay et al. 1989), was consistent with an ~10 kDa protein, and therefore confirmed its monomeric state. The chemical shift dispersion of the amide resonances in both ^{1}H and ^{15}N dimensions was characteristic of a folded protein in solution (Fig. 1).

The extensive and accurate assignment of the backbone and side chain ^{1}H, ^{13}C and ^{15}N chemical shifts (99 % of backbone and 93 % of side chain resonances were assigned) were crucial as initial experimental input for the automatic assignment of NOESY peaks during the iterative structure calculations using CYANA. The agreement of the final assigned 1863 NOESY peaks from the 3D NOESY spectra and the calculated structures were verified by RPF software package (Huang et al. 2005). Good convergence was observed, as indicated in Table 1. Figure 2a shows the

Table 1 Structure statistics for the C-terminal domain of CV_0373 protein[a]

Conformationally-restricting restraints[b]	
Distance restraints	
Intra-residue (i = j)	207
Sequential (li-jl = 1)	238
Medium-range (1 < li–jl < 5)	85
Long-range (li–jl ≥ 5)	333
Total	1,863
Hydrogen bond restraints	
Long-range (li–jl ≥ 5)/total	12/58
Dihedral angle restraints	104
NH RDC restraints (Peg/Gel)	42/49
Residue restraint violations[b]	
Average number of distance violations per structure	
0.1–0.2 Å	4
0.2–0.5 Å	1
>0.5 Å	0
Average RMS distance violation/restraint (Å)	0.01
Maximum distance violation (Å)	0.28
Average number of dihedral angle violations per structure	
1–10°	0.9
>10°	0
Average RMS dihedral angle violation/restraint (degree)	0.2
Maximum dihedral angle violation (degree)	3.3
RDC Q_{RMSD} (Peg/Gel)	0.45/0.26
RMSD from average coordinates[b,c]	
Backbone/Heavy atoms (Å)	0.5/0.9
Molprobity Ramachandran plot statistics[b,c]	
Most favored regions (%)	97.8
Allowed regions (%)	2.0
Disallowed regions (%)	0.2
Global quality scores (raw/Z-score)[b]	
Verify3D	0.33/−2.09
Prosall	0.41/−0.99
Procheck(phi-psi)[c]	0.20/1.10
Procheck(all)[c]	0.20/1.18
Molprobity clash	16.85/−1.37
RPF scores[d]	
Recall	0.97
Precision	0.90
F-measure	0.95
DP-score	0.81

[a] Structure statistics were computed for the ensemble of 20 deposited structures

[b] Calculated using PSVS 1.4 program. Residues (175–257) were analyzed

[c] Ordered residues ranges (with sum of phi and psi >1.8): 181–194, 200–212, 218–221, 226–232, 236–253

[d] RPF scores reflected the goodness-of-fit of the final ensemble of structures including disordered residues to the NMR data

superposition of the ordered regions of the final ensemble of 20 calculated structures, which have a RMSD of 0.5 Å for backbone atoms and 0.9 Å for heavy atoms.

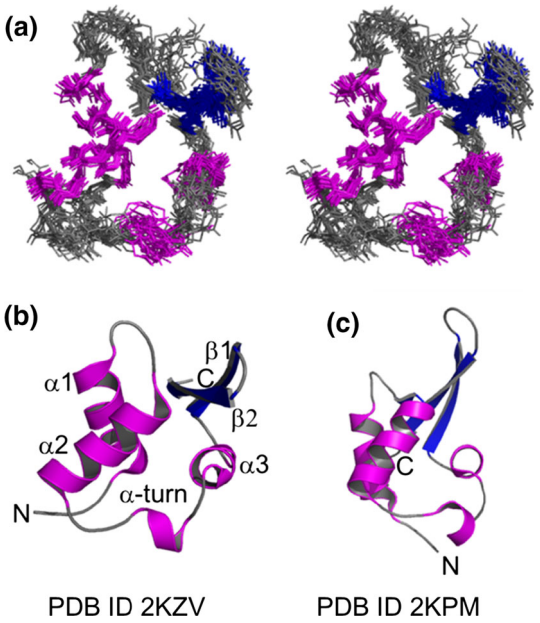

Fig. 2 **a** Stereoview of the superimpositions of the 20 lowest energy structures of CV_0373 CTD. The three α-helices are colored magenta, two β-strands colored *blue*, and the N-terminal tail, C-terminal tail and loop regions are colored *grey*. The first two residues in N-terminus and C-terminal hexaHis tags (LEHHHHHH) are not shown for clarity. **b** Ribbon diagram of the lowest energy structure of CV_0373 CTD. All secondary structural elements are labeled. **c** Ribbon diagram of NE_0665 CTD from *Nitrosomonas europaea*

Figure 2b shows a ribbon representation of the lowest energy structure of CV_0373 CTD from the ensemble. All secondary elements in ensemble were well defined including the three helices colored magenta (α1: L182-V193, α2: L202-N212, and α3: R225-K231) and the two strands colored blue (β1: L236-N243, β2: K246-L253). There is a small 3_{10} α-helix (P218-W221) between α2 and α3. CV_0373 CTD adopts a typical wHTH fold composed of three helices with a C-terminal extension of two anti-parallel β-strands.

Discussion and conclusions

A sequence profile search using the sequence of CV_0373 CTD as a query by PSI-BLAST revealed no similar proteins with known structures except for the C-terminal domain of NE0665 (174–269) from *Nitrosomonas europaea* (referred to as NE0665 CTD, PDB ID 2KPM). NE0665 CTD is a homolog of CV_0373 CTD sharing 44 % sequence identity, whose solution structure was also solved by NESG (NESG ID NeR103A) as another target for structure determination for the OST–HTH/LOTUS domain family. The solution structure of NE0665 CTD (Fig. 2c) also adopts a wHTH fold and exhibits a high overall structure similarity to CV_0373, except for one small β-strand between α1 and α2. Both wHTHs share

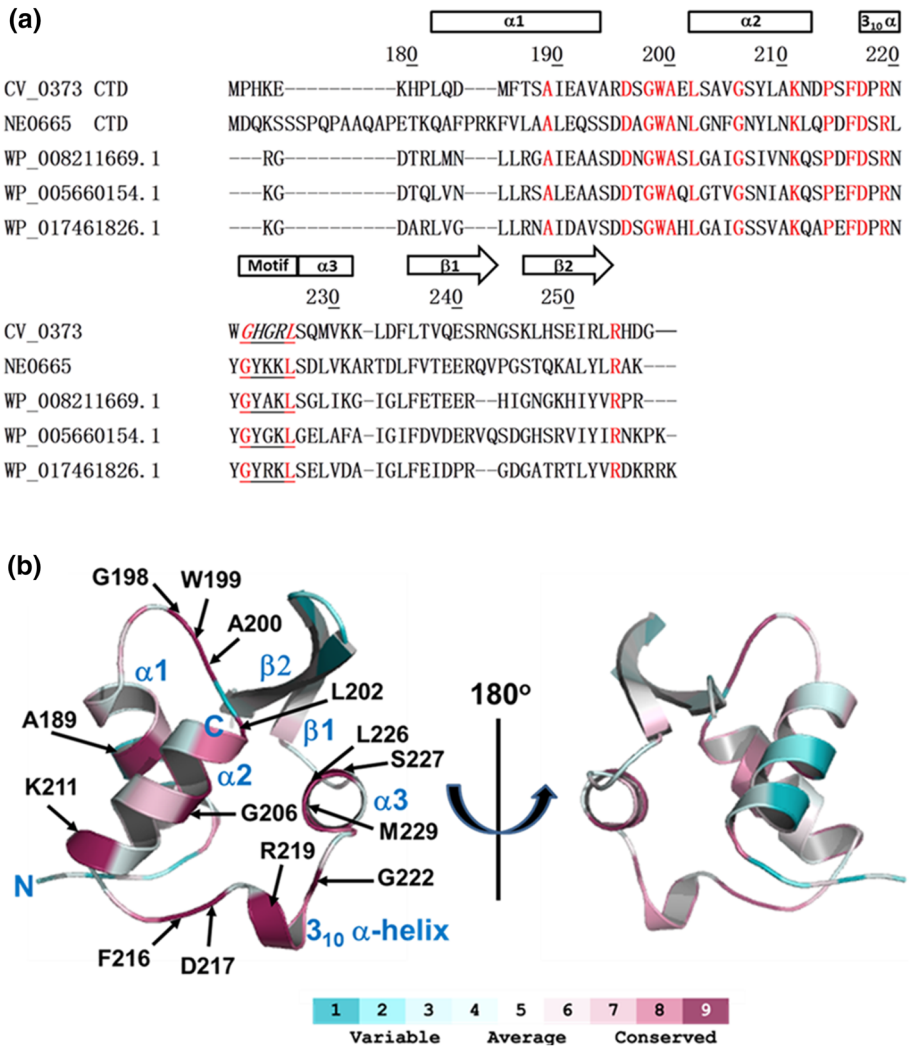

Fig. 3 **a** Multiple amino acid sequence alignments of OST–HTH domain in various organisms performed using clustalw2 (http://www.ebi.ac.uk/Tools/msa/clustalw2/). Proteins from five different organisms are shown here including CV_0373 CTD from *C. violaceum*, NE0665 CTD from *Nitrosomonas europaea*, WP_008211669.1 (GI: 495486984) from *Rhodanobacter* sp. 115, WP_017461826.1 (GI:516031243) from *Dyella ginsengisoli*, WP_005660154.1 (GI:491899744) from *Dethiosulfovibrio peptidovoran*. Secondary structural elements of CV_0373 CTD and sequence motif (Ghxph) are indicated. Highly conserved residues based on ConSurf analysis are color *red*. ConSurf analysis was performed using the first structure of CV_0373 CTD (PDB ID 2KZV, chain A) as a query for homologs search with an E-value cut-off of 0.0001, maximal and minimal sequence identity of 95 and 35 %, PSI-BLAST iteration number of three using a non-redundant sequence data bank. 40 unique sequences out of 47 PSI-BLAST hits were used for the conservation score calculation. **b** Amino acid conservation mapped onto the lowest energy NMR structure based on ConSurf analysis. Conserved residues are indicated using *pink*, *red*, or *magenta*

a distinct extended insert including five residues following the short 3_{10} α-helix between the α2 and α3, which is a defining sequence motif for the OST–HTH domain, namely a conserved Ghxph motif (where h is hydrophobic, x is any residue and p is polar). The sequence motif for the CV_0373 CTD is GHGRL (residues 222–226) after the 3_{10} α-helix (PRNW, 218–221) compared to GYKKL (residues 234–238) after the 3_{10} α-helix (SRLY, 230–233) for the NE0665 CTD (Fig. 3a). This insert in NE0665 CTD has been claimed as a unique structural feature of OST–HTH domains compared to all other wHTHs (Anantharaman et al. 2010). In their study, a structure similarity search for NE0665 CTD using the DALI program revealed that the best hit was the wHTH domain of the archaeal replication protein CDC6 that binds dsDNA. On the basis of the superposition on the CDC6 wHTH-dsDNA co-crystal structure, they inferred that in addition to the possible dsRNA minor groove contacts by the tip of the 'wing' and major groove contacts by α3, the unique insert of NE0665 CTD could also contact a second minor groove, distinct from the one contacted by the wing.

ConSurf analysis (Ashkenazy et al. 2010; Glaser et al. 2003) based on five related sequences (Fig. 3a) showed

that 14 amino acids have the highest conservation score (9) for the domain family as indicated in Fig. 3b. All these residues are present on one side of solution structure, and entirely located in the helix-turn-helix core region (left panel, Fig. 3b). The unique insert region between α2 and α3 mentioned before (including the Gpxph sequence motif) is conserved. By contrast, conserved residues are relatively absent on α1 (A189) and α2 (G206 and K211), whereas conserved residues are found on loop 1 (G198, W199, A200 and L202), loop 2 (F216, D217, R219 and G222), and α3 (L226, S227, M229) indicating that these residues could play a key role in the function of this domain, such as dsRNA binding.

The neighboring genes surrounding CV_0373, including CV_0371, CV_0374 and CV_0375, encode hypothetical proteins (http://www.kegg.jp/kegg-bin/show_genomemap?ORG=cvi&ACCESSION=CV_0373), except for CV_0372, which encodes for phosphinothricin acetyltransferase, an enzyme that catalyzes the chemical reaction between acetyl-CoA and phosphinothricin by producing CoA and *N*-acetylphosphinothricin. Acetyl-CoA is an important molecule in metabolism used in many biochemical reactions with its main function serving to convey the carbon atoms within the acetyl group to the citric acid cycle to be oxidized for energy production. By comparisons with the putative diverse functions of eukaryotic OST–HTH domains (Anantharaman et al. 2010), bacterial homologs such as CV-0373 CTD that are fused to N-terminal NYN domains might serve as standalone RNA-degradation enzymes (Anantharaman et al. 2010).

Acknowledgments This work was supported by the National Institute of General Medical Sciences; Protein Structure Initiative-Biology Program; Grant Number: U54-GM074958 and U54-GM094597. We thank D. Wang, C. Ciccosanti, L. Mao, H. Janjua, and T. Acton at the Rutgers protein production facility for technical support. All NMR data collection, except for RDCs, was conducted at the Ohio Biomedicine Center of Excellence in Structural Biology and Metabonomics at Miami University.

References

Acton TB, Xiao R, Anderson S, Aramini J, Buchwald WA, Ciccosanti C, Conover K, Everett J, Hamilton K, Huang YJ, Janjua H, Kornhaber G, Lau J, Lee DY, Liu G, Maglaqui M, Ma L, Mao L, Patel D, Rossi P, Sahdev S, Shastry R, Swapna GV, Tang Y, Tong S, Wang D, Wang H, Zhao L, Montelione GT (2011) Preparation of protein samples for NMR structure, function, and small-molecule screening studies. Methods Enzymol 493:21–60

Anantharaman V, Aravind L (2006) The NYN domains: novel predicted RNAses with a PIN domain-like fold. RNA Biol 3:18–27

Anantharaman V, Zhang D, Aravind L (2010) OST–HTH: a novel predicted RNA-binding domain. Biol Direct 5:13

Ashkenazy H, Erez E, Martz E, Pupko T, Ben-Tal N (2010) ConSurf 2010: calculating evolutionary conservation in sequence and structure of proteins and nucleic acids. Nucleic Acids Res 38:W529–W533

Bhattacharya A, Tejero R, Montelione GT (2007) Evaluating protein structures determined by structural genomics consortia. Proteins 66:778–795

Brazilian National Genome Project C (2003) The complete genome sequence of *Chromobacterium violaceum* reveals remarkable and exploitable bacterial adaptability. Proc Natl Acad Sci USA 100:11660–11665

Cai ML, Huang Y, Suh JY, Louis JM, Ghirlando R, Craigie R, Clore GM (2007) Solution NMR structure of the barrier-to-autointegration factor-emerin complex. J Biol Chem 282:14525–14535

Callebaut I, Mornon JP (2010) LOTUS, a new domain associated with small RNA pathways in the germline. Bioinformatics 26:1140–1144

Glaser F, Pupko T, Paz I, Bell RE, Bechor-Shental D, Martz E, Ben-Tal N (2003) ConSurf: identification of functional regions in proteins by surface-mapping of phylogenetic information. Bioinformatics 19:163–164

Guntert P (2004) Automated NMR structure calculation with CYANA. Methods Mol Biol 278:353–378

Hansen MR, Mueller L, Pardi A (1998) Tunable alignment of macromolecules by filamentous phage yields dipolar coupling interactions. Nat Struct Biol 5:1065–1074

Huang YJ, Powers R, Montelione GT (2005) Protein NMR recall, precision, and F-measure scores (RPF scores): structure quality assessment measures based on information retrieval statistics. J Am Chem Soc 127:1665–1674

Kay LE, Torchia DA, Bax A (1989) Backbone dynamics of proteins as studied by 15 N inverse detected heteronuclear NMR spectroscopy: application to *staphylococcal* nuclease. Biochemistry 28:8972–8979

Kodach LL, Bos CL, Duran N, Peppelenbosch MP, Ferreira CV, Hardwick JC (2006) Violacein synergistically increases 5-fluorouracil cytotoxicity, induces apoptosis and inhibits Akt-mediated signal transduction in human colorectal cancer cells. Carcinogenesis 27:508–516

Neri D, Szyperski T, Otting G, Senn H, Wuthrich K (1989) Stereospecific nuclear magnetic resonance assignments of the methyl groups of valine and leucine in the DNA-binding domain of the 434 repressor by biosynthetically directed fractional 13C labeling. Biochemistry 28:7510–7516

Ruckert M, Otting G (2000) Alignment of biological macromolecules in novel nonionic liquid crystalline media for NMR experiments. J Am Chem Soc 122:7793–7797

Schwieters CD, Kuszewski JJ, Clore GM (2006) Using Xplor-NIH for NMR molecular structure determination. Prog Nucl Magn Reson Spectrosc 48:47–62

Shen Y, Delaglio F, Cornilescu G, Bax A (2009) TALOS plus: a hybrid method for predicting protein backbone torsion angles from NMR chemical shifts. J Biomol NMR 44:213–223

Tjandra N, Grzesiek S, Bax A (1996) Magnetic field dependence of nitrogen-proton J splittings in N-15-enriched human ubiquitin resulting from relaxation interference and residual dipolar coupling. J Am Chem Soc 118:6264–6272